4ICEGE Thessaloniki-GREECE 2007

4th International Conference on
Earthquake Geotechnical Engineering
June 25-28, 2007
Paper No. 1452

SUPPLEMENTATION TORSIONAL FORCED VIBRATION MODEL FOR FIXED-FREE RESONANT COLUMN TEST

Man T. Bui [1]

ABSTRACT

The single-degree-of-freedom (SDOF) forced torsional vibration model is supplemented to take into account the effect of imperfect fixity and deformation of the fixed-free resonant column (RC) equipment. A torsional spring with a finite stiffness was introduced to the imperfect fixed-free RC test, forming a new system termed 'spring-base' fixed-free RC configuration, which is assumed to be equivalent to the perfect fixed-free RC configuration. The equivalent system is assumed SDOF. The behaviour of the specimen at small strain is described by the Kelvin-Voigt model. Solutions of the model are derived dependently on types of transducer monitoring motion of the free end. Based on relationship between the natural frequency and shear stiffness of specimen, a new formula for calculation shear wave velocity, V_S, of the specimen are derived. The solutions of the model are simple in use and comparable to those of other models. In addition, an exact expression of half power point (HPP) method, a new method of calibration the moment of inertia of the driving system and the equipment stiffness are suggested.

Keywords: small strain stiffness, shear wave, resonant column, half power point method, viscoelastic

INTRODUCTION

Due to the simplicity of equipment and data reduction technique, the fixed-free (Fig. 1b) is the most popular type of RC apparatus for determination dynamics properties of soil (Drnevich, 1985). The fixed-free RC apparatus works with the boundary condition that one end (called the free end) of the specimen is free to move and the other end (called the fixed end) is fixed. So that neither movement nor deformation of the equipment is allowed. Normally, to reduce the equipment displacement/ deformation, the equipment needs to be firmly fixed to a very heavy mass (e.g. anchored to a concrete floor) and the equipment stiffness should be much higher than that of the specimen.

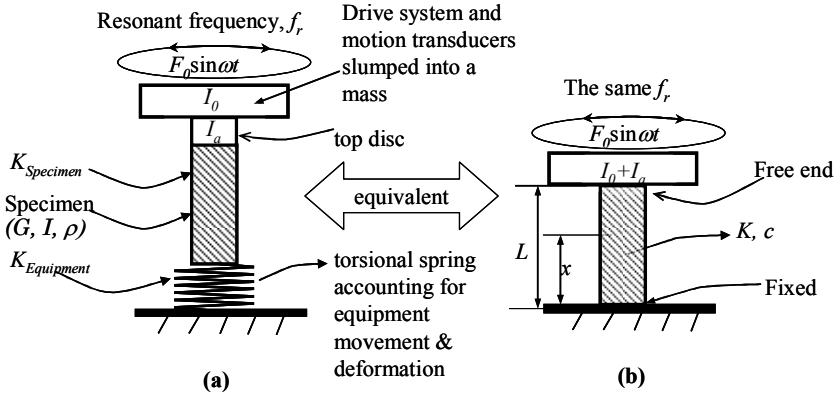

Figure 1. Schematic of (a) imperfect fixed-free RC test, and (b) the equivalent fixed-free RC test

[1]PhD Student, School of Civil Engineering and the Environment, University of Southampton, United Kingdom, Email: man.bui@soton.ac.uk

Although there is no constitutive model that can describe the small strain behaviours of soil specimen under all loading condition in RC test, wave propagation in the linear viscoelastic circular rod was suggested to be the good model (Hardin, 1965). The analytical solutions for soil sample not subjected to any ambient state of stress (with various cases of boundary conditions) were presented in detail by Hardin (1965), Hardin and Music (1965), and Drnevich et al. (1978). However, the derivation, solutions, and procedure of data reduction are rather complicated.

Hall and Richart (1963) and Richart et al. (1970) suggested that the small strain behaviours of soil in RC apparatus can be also described by linear elastic model, which ignores the viscous damping, and implicitly implies that the input energy produced by driving system is used for maintaining the harmonic motion and hence the shear wave propagates at natural frequency (normal mode). The beauty of elastic model is its simple solution, enabling to accurately estimate shear wave velocity V_s of low damping soil. In reality, the input energy is not only for compensation the energy lost but changing the vibratory amplitude as well. Nevertheless, the elastic model cannot provide information relevant to measured peak vibratory amplitude. It is inevitable that the solution of the elastic model has certain error increasing with damping, which in turn increases with shear strain. Furthermore, it cannot establish itself a tool (but employed the decay vibration or HPP method derived from force torsional vibration model) for estimation damping ratio, D. It is great if a formula for calculation shear wave velocity, a relationship between input energy and peak amplitude, and tools for estimation damping ratio are gathered in a simple model.

Due to imperfect fixity and deformation of test equipment, compliance issues have been encountered in RC test. Avramidis and Saxena (1990) found that the stiffness of their original RC equipment was insufficient to test stiff specimens such as cemented sand. Thus, their original equipment was stiffened. Consequently, G_{max} of the Monterey N^{o}0 sand measured by the modified equipment were up to 28% higher, and damping ratios were up to five times lower than those measured by the original apparatus. Priest (2004) observed movement of the base of aluminium bar N^{o}4, a relative high stiff specimen, suggesting that the assumptions of a fixed base and SDOF system could be failed. Consequently, the moment of inertia of the driving system, I_0, was not a constant but increased with stiffness and hence resonant frequency, f_r, of calibration bars. To eliminate the dependency of I_0 on f_r, a relationship between I_0 and f_r was suggested (Clayton et al., 2005, Priest, 2004). Cascante et al. (2003) reported that the maximum displacement of the base greatly increased with stiffness of aluminium rod. Thus to reduce the effect of the movement of the base, their RC equipment was fixed to a heavy steel frame. They mentioned further that energy discharged due to the movement of the base requires further investigation.

In this paper, to take into account the effect of the equipment compliance, a torsional spring with a finite stiffness, $k_{equipment}$, was introduced to the imperfect fixed-free RC test, forming a new system termed 'spring-base' fixed-free RC configuration (Fig. 1a), which is assumed to be equivalent to the perfect fixed-free RC configuration (Fig. 1b). The behaviour of the specimen at small strain is described by the Kelvin-Voigt model. The simplicity of the boundary conditions of the perfect fixed-free RC apparatus suggests that the analytical solutions can be simply derived from the SDOF torsional forced vibration model. The solutions of the model are derived dependently on types of instrumented motion transducers (i.e. proximeter, velocimeter, or accelerometer). The solutions applied for a proximeter are presented in detail in a textbook, and this paper supplements the solutions applied for a velocimeter and particularly for an accelerometer that is usually instrumented in the RC apparatus. Consequently, the simple formula for calculating shear wave velocity, the exact expression of HPP method, and the new method for calibration equipment stiffness and moment of inertia of the driving system are suggested.

SUPPLEMENTATION SDOF TORSIONAL VIBRATION MODEL

Governing equation and general solution for accelerometer

The governing equation is established with the following assumptions:

- I_0 is constant, dependently on geometry and density of the driving system only, and it is independent on stiffness of specimen.
- The imperfect fixity of the base and deformation of test equipment can be represented by a spring with a finite torsional stiffness, $K_{equipment}$.
- The equivalent system is SDOF.
- The equivalent specimen is viscoelastic material with the equivalent stiffness, K, calculated as:

$$\frac{1}{K} = \frac{1}{K_{equipment}} + \frac{1}{K_{specimen}} \tag{1}$$

- The shear strain in the equivalent specimen varies linearly to the distant x from the fixed end (or the angle of twist per unit length is constant). The validity of this assumption will be presented in the discussion section.

Based on the above assumptions, the governing equation of SDOF torsional forced vibration of a viscoelastic specimen is (see more detail in the appendix A):

$$I_0 \frac{\partial^2 \theta}{\partial t^2} + c \frac{\partial \theta}{\partial t} + k\theta = F_0 \sin \omega t \tag{2}$$

In RC apparatus the motion of the free end is normally monitored by an accelerometer; and the output acceleration amplitude, as the solution of Equation (2), is a harmonic function having the general form below (if damping is less than the critical damping):

$$\frac{\partial^2 \theta}{\partial t^2} = A \sin(\omega t + \pi - \psi) = -\omega^2 \theta \tag{3}$$

In which,

$$A = \frac{F_0 \omega^2}{\sqrt{\left(k - I_0 \omega^2\right)^2 + (c\omega)^2}} \tag{4}$$

$$\cos\psi = \frac{\left(k - I_0 \omega^2\right)}{\sqrt{\left(k - I_0 \omega^2\right)^2 + (c\omega)^2}} \tag{5}$$

Equations (3), (4) and (5) are the basic solutions, from which further data-reduction formulae are derived.

Relationship between V_S and natural/ resonant frequency

Equation (5) indicates that the angle Ψ equal 90 degrees (or Lissajous figure is a right ellipse) if $k - I_0 \omega^2 = 0$, or vibratory frequency coincides with the natural frequency:

$$\omega = \sqrt{\frac{k}{I_0}} = \omega_0 \tag{6}$$

Submission Equation (1) to Equation (6) leads to:

$$\frac{1}{K_{specimen}} = \frac{1}{I_0 \omega_0^{\ 2}} - \frac{1}{K_{equipment}} \tag{7}$$

Since the shear stiffness of the specimen is defined by Equation (A4) (in the appendix), the shear modulus G of the specimen can be calculated by the following formula:

$$G = \frac{k_{specimen} L}{I_p} = \frac{L \omega_0^{\ 2} I_0}{I_p} \times \left(1 - \frac{\omega_0^{\ 2} I_0}{K_{equipment}} \right)^{-1} \tag{8}$$

In which, L is the length and I_p is the area polar moment of inertia of circular cross section of the specimen. Accordingly, a new equation for calculation shear wave velocity of the specimen is derived:

$$V_s = \sqrt{\frac{G}{\rho}} = \omega_0 L \sqrt{\frac{I_0}{I}} \left(1 - \frac{\omega_0^{\ 2} I_0}{K_{equipment}} \right)^{-0.5} \tag{9}$$

In Equation (9), I is the moment of inertia of the specimen, $I = \rho I_P L$. Denote α_r is the ratio of the resonant frequency to the natural frequency. Equation (9) can be rewritten as:

$$V_s = \frac{\omega_r L}{\alpha_r} \sqrt{\frac{I_0}{I}} \left(1 - \frac{\omega_0^{\ 2} I_0}{K_{equipment}} \right)^{-0.5} \tag{10}$$

The formula of α_r will be derived in the next section (Equation 12). It was mentioned that data derived from maximum amplitude technique is less effective than those from phase relationship (Drnevich, 1985). In practice, the natural frequency can be achieved manually by adjusting Lissajous figure, and the resonant frequency can be determined quickly and precisely by analysis frequency response curve with an aid of a data acquisition system and a software. The Equations (9) and (10) above suggest that V_s can be accurately derived by both techniques.

Relationship between natural and resonant frequency

At shown in appendix A, the vibratory acceleration amplitude attains the maximum value if:

$$\omega = \frac{\omega_0}{\sqrt{1 - 2D^2}} = \omega_r \tag{11}$$

Therefore, the ratio of the resonant frequency to the natural frequency, α_r, is determined as:

$$\alpha_r = \frac{\omega_r}{\omega_0} = \frac{1}{\sqrt{1 - 2D^2}} \tag{12}$$

In addition, Equation (12) can be also rearranged as:

$$\omega_r = \sqrt{\frac{k}{I_0 (1 - 2D^2)}} = \sqrt{\frac{k}{I_0 - I_c}} \tag{13}$$

In Equation (13), I_c can be termed the damping moment of inertia of the system, $I_c = 2D^2 I_0$. It is a virtual mass polar moment of inertia. An equation similar to Equation (13) was derived by Li et al., (1998) via different approach.

Exact solution of half power point method

Damping ratio of soil specimen tested by RC apparatus can be estimated by HPP method. However, this method is an approximation, and the error increases with the damping ratio (Fig. 2), especially at medium to large strain where the damping ratio can excess 10%. Hence, if the damping ratio of soil is high, an exact formula of HPP is required. As shown in the appendix A, the exact formula of HPP method is:

$$\frac{f_2 - f_1}{2f_r} = \frac{1}{\alpha_r}\sqrt{\frac{\alpha_r^{\,2} - \sqrt{2\alpha_r^{\,4} - 1}}{2\left(2\alpha_r^{\,4} - 1\right)}} \tag{14}$$

In which, f_1 and f_2 are frequencies at which acceleration amplitudes equal to 0.7171 times the peak amplitude. Equation (14) is plotted in Fig. 2, which can be employed to quick estimation damping ratio e.g. if the expression in the left hand side of Equation (14) is 16%, the figure gives D = 13%.

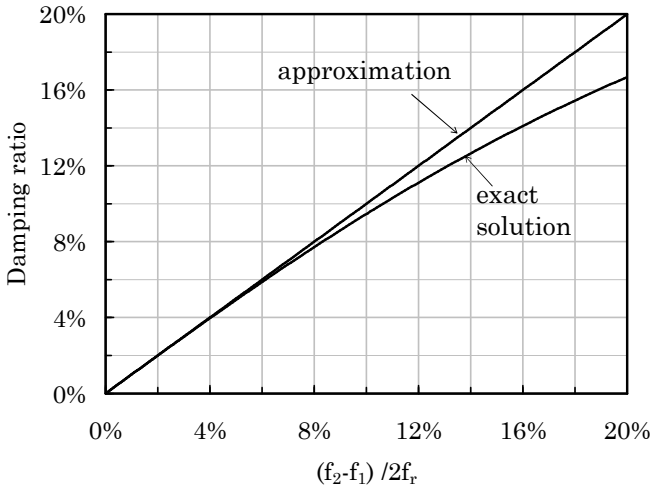

Figure 2: Exact solution of HPP method

Solutions for velocimeter and proximeter

The solutions for the cases of velocimeter and proximeter instrumented in fixed-free RC apparatus can be derived similarly, and they are summarised in Table 1. It is noted that the resonant frequency, which causes maximum velocity amplitude, coincides with the natural frequency (α_r = 1). As a result, the data reduced from the velocimeter is simpler.

Table 1: Main Solutions of torsional vibration model

Motion transducer	Ratio of resonant frequency to natural frequency, α_r	Shape of Lissajous figure	Shear wave velocity, V_s
Accelerometer	$\frac{1}{\sqrt{1-2D^2}} > 1$	Right ellipse	$V_s = \omega_0 L\sqrt{\frac{I_0}{I}}\left(1 - \frac{\omega_0^{\,2} I_0}{K_{equipment}}\right)^{-0.5}$
Velocimeter	unity	Slope line	
Proximeter	$\sqrt{1-2D^2} < 1$	Right ellipse	

CALIBRATION $K_{EQUIPMENT}$ AND I_0

The two equipment parameters, $K_{equipment}$ and I_0, can be determined using experimental method. The calibration method is based on Equation (7), which is explicitly rewritten as:

$$\frac{1}{K_{specimen}} + \frac{1}{K_{disc}} = \left(\frac{1}{I_0 + I_a}\right)\frac{1}{\omega_0^2} - \frac{1}{K_{equipment}} \tag{15}$$

In which, K_{disc} is shear stiffness of the top disc of a calibration bar. Equation (15) expresses a linear relationship between $\left(1/K_{specimen} + 1/K_{disc}\right)$ and $1/\omega_0^2$. In this relationship, $1/(I_0 + I_a)$ is a slope of the line and $1/K_{equipment}$ is the *Y*-intercept (Fig. 3). Hence, a series of calibration bars with different diameter need to be tested to establish the linear relationship between $1/K_{specimen}$ and $1/\omega_0^2$. Via regressive analysis, the slope of the line and the *Y*-intercept will be acquired. Hence, both I_0 and $K_{equipment}$ will be determined.

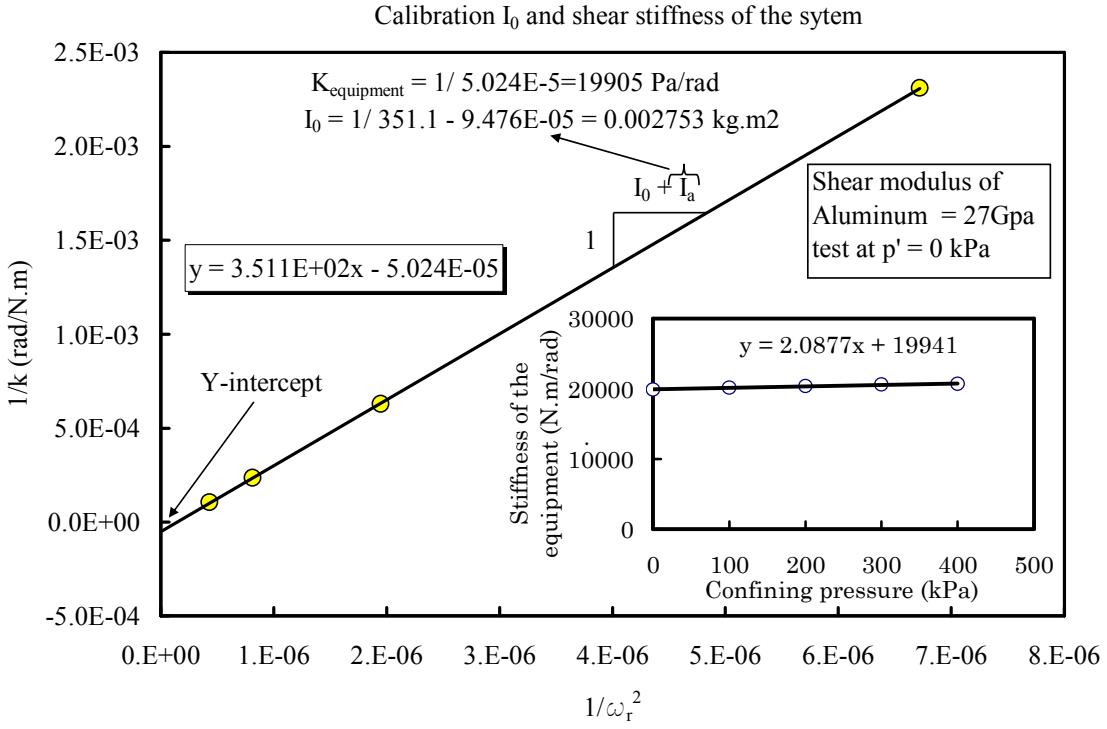

Figure 3: Calibration I_0 and $K_{equipment}$

An example of calibration I_0 and $K_{equipment}$ of a RC apparatus was presented in Fig. 3. In this calibration, the resonant frequencies of each aluminium bar were measured at several small strains, from $3 \div 4 \times 10^{-5}\%$ to $1 \times 10^{-4}\%$. The resonant frequencies of each aluminium bar in this strain range were very consistent (the variations in resonant frequencies were not more than 0.1 Hz). Then, the resonant frequencies were averaged. To check the consistency, the above calibration process was repeated at different confining pressures. It is observed that this calibration technique yields a constant I_0, and $K_{equipment.}$, lightly linearly increasing with confining pressure (see the inset in Fig. 3).

DISSCUSSION

Solutions of the SODF torsional vibration model (Fig. 1b) are comparable to those of viscoelastic model (Hardin, 1965) and elastic model (Richart et al., 1970). The model can be considered as a special case of the wave propagation in a viscoelastic circular rod with the specific assumption that the mode shape is a straight line (Fig. 4a). Based on this assumption, Equations (A2, A4) in the appendix A were established, and subsequently the velocity Equation (9) was derived. Based on the governing equation of wave propagating in elastic rod, Richart et al. (1970) suggested that the first mode shape of the fixed-free elastic rod is more general (the angle of twist per unit length is not constant, Fig. 4b), and they derived the following equation:

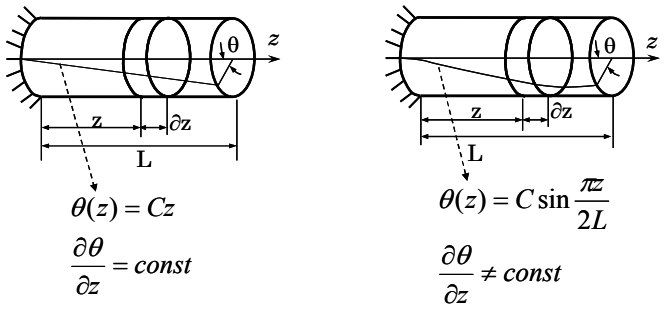

(a) SDOF torsional forced vibration **(b) Elastic wave model**

Figure 4: Mode function

$$\frac{I}{I_0} = \frac{\omega_0 L}{V_s} \tan \frac{\omega_0 L}{V_s} \tag{17}$$

If the stiffness of the equipment is infinite, and if damping ratio is small, Equation (10) can be simplified as:

$$\beta = \frac{\omega_0 L}{V_s} = \sqrt{\frac{I}{I_0}} \tag{18}$$

Submission Equation (18) into Equation (17) leads to:

$$\sqrt{\frac{I}{I_0}} = \tan \sqrt{\frac{I}{I_0}} \tag{19}$$

Equation (19) requires the ratio I/I_0 tends to infinitesimal. Study the wave propagation in a viscoelastic circular rod, Hardin (1965) explained that the higher resonances (higher normal mode) are damped out when damping increased, and that the system approach SDOF (fixed-free configuration) if the ratio I/I_0 become infinitesimal. This condition and the condition (19) are identical. The SDOF torsional vibration model can practically meet this condition if the moment of inertia of the driving system is much larger than that of soil specimen.

Whether the shear wave velocity calculated by SDOF torsional vibration model is comparable to that calculated by other models such as viscoelastic model (Hardin, 1965) and elastic model (Richart et al., 1970) will depend on how in reality the condition (19) is satisfied. The spring-base viscoelastic model was employed to calculate G_{max} of some solid cylindrical sand specimens, which were approximately 7 cm in diameter and 14 cm in height. For comparison, G_{max} of these specimens were then calculated by elastic model (Richart et al. 1970) combined with the concept that I_0 is dependent on resonant

frequency (Clayton et al. 2005; Priest, 2004). The ratio I/I_0 of these specimens varied from 0.15 to 0.18. So that the condition (19) cannot be well satisfied. The error of condition (19) is from 5% to 6% (e.g. if $I/I_0 = 0.18, \sqrt{I/I_0} = 0.42$, and $tan\sqrt{I/I_0} = 0.45$), leading to a small difference in calculation G_{max}. The results were plotted in Fig. 5 showing that there were differences in G_{max} calculated by two methods; however they were negligible (less than 5%). It is noted that the initial damping ratio, $D_{min,}$ of all tested material were lower than 1%.

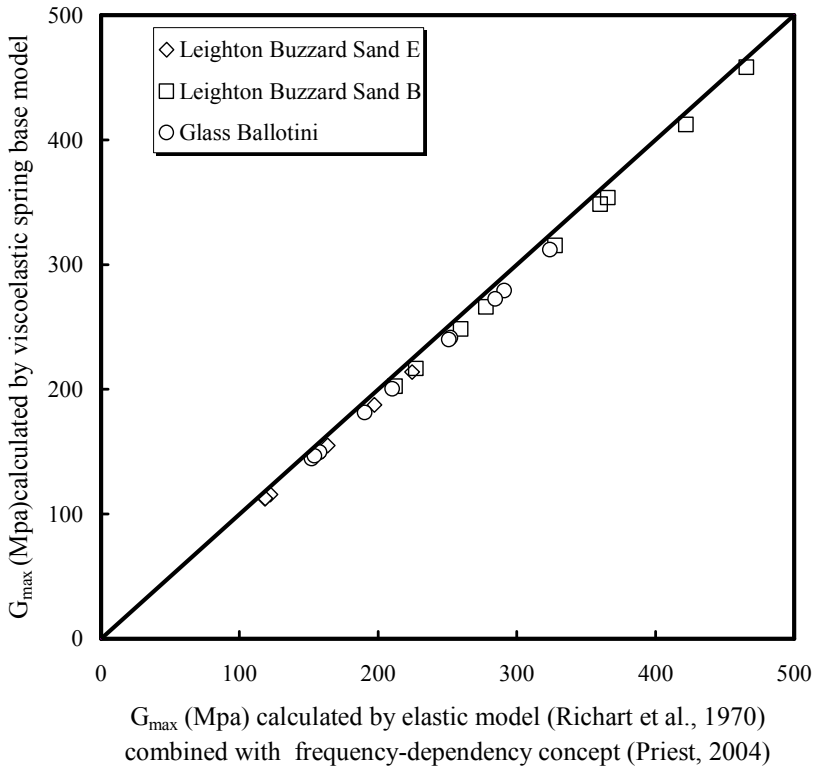

Figure 5: Comparison G_{max}, determined by spring base model and elastic model (Richart and Hall, 1970) combining with frequency dependency concept

In addition, Equation (10) is very convenient in used, especially when dealing with a large number of calculation, since it can be quickly performed in a worksheet. In contrast, Equation (17) need to be solved using a trial method (e.g. using the gold seek tool built in MS Excel), and the viscoelastic model (Hardin, 1965) required a software (e.g. ASTM-D4051, 1995). If the amount of calculation is numerous, these methods are time consuming.

CONCLUSION

The SDOF torsional forced vibration model is expended to take into account the effects of the equipment compliance. The model gathers: (1) the explicit relationship between measured peak vibration amplitude and other parameters e.g. damping ratio, harmonic force, (2) the simple formulae for calculation shear modulus, and (3) the methods for estimation damping ratio. The solutions of the model are simple in use and comparable to those of other models. Hence the model is suggested to be suitable for fixed-free RC test.

ACKNOWLEDGEMENT

The author would like to express his deep gratitude to Professor C.R.I. Clayton, and Dr. Jeffrey A. Priest, senior research fellow, School of Civil Engineering and the Environment, University of Southampton, for many valuable discussions.

APPENDIX A

Since the system is SDOF, only the torsional vibration of the free end is considered. The applied harmonic torque $F_0 \sin \omega t$ causes in the cross section at the free end a shear stress proportional to the radial distant r from the axis:

$$\tau = G\gamma + \mu \frac{\partial \gamma}{\partial t} = G\left(r\frac{\theta}{L}\right) + \mu \frac{\partial\left(r\frac{\theta}{L}\right)}{\partial t} \tag{A1}$$

Where γ is the shear strain, and μ are the viscosity of the equivalent specimen. Equation (A1) was established with the assumption that the angle of twist per unit length is constant. Thus, the total resisting torque about the axis of the rod is the summation of element moments:

$$T = \int \tau (dA) r = G\frac{\theta}{L}\int r^2 dA + \frac{\mu}{L}\frac{\partial \theta}{\partial t}\int r^2 dA = \frac{GI_p}{L}\theta + \frac{\mu I_P}{L}\frac{\partial \theta}{\partial t} \tag{A2}$$

Where dA is an element at the radial distant r from the axis. The motion of the rod is absorbed by a damping force, assumed to be proportional to the angular velocity of the slumped mass. The equilibrium condition of the slumped mass yields the governing equation of SDOF torsional forced vibration:

$$I_0 \frac{\partial^2 \theta}{\partial t^2} + \frac{\mu I_P}{L}\frac{\partial \theta}{\partial t} + \frac{GI_p}{L}\theta = F_0 \sin \omega t \tag{A3}$$

Denote:

$$k = \frac{GI_p}{L} \tag{A4}$$

$$c = \frac{\mu I_P}{L} \tag{A5}$$

In which, c is the damping coefficient. Equation (A3) is simplified as:

$$I_0 \frac{\partial^2 \theta}{\partial t^2} + c\frac{\partial \theta}{\partial t} + k\theta = F_0 \sin \omega t \tag{A6}$$

Equation (A6) is a familiar governing equation SDOF torsional vibration. As a solution of Equation (A6), the output acceleration amplitude has the general form:

$$\frac{\partial^2 \theta}{\partial t^2} = A\sin(\omega t + \pi - \psi) \tag{A7}$$

In which,

$$A = \frac{F_0 \omega^2}{\sqrt{\left(k - I_0 \omega^2\right)^2 + \left(c\omega\right)^2}} \tag{A8}$$

By denoting:

$$x = \left(\frac{\omega}{\omega_0}\right)^2 \tag{A9}$$

$$D = \frac{c}{\sqrt{4kI_0}} = \frac{c}{2I_0\omega_0} = \frac{\mu I_p}{2I_0\omega_0 L} \tag{A10}$$

Equation (A8) is simplified as:

$$A = \frac{F_0}{I_0} \times \frac{x}{\sqrt{(1-x)^2 + 4D^2 x}} \tag{A11}$$

Equation (A11) indicates the accelerative vibratory amplitude, *A,* is a function of vibratory frequency, the specimen stiffness, and the harmonic force. Derivative Equation (A12) with respect to *x:*

$$\frac{\partial A}{\partial x} = \frac{F_0}{I_0} \frac{1 - x\left(1 - 2D^2\right)}{\left[(1-x)^2 + 4D^2 x\right]^{3/2}} \tag{A12}$$

Thus, at resonance we have:

$$x = x_r = \frac{1}{1 - 2D^2} \text{ or } \omega_r = \frac{\omega_0}{\sqrt{1 - 2D^2}} > \omega_0 \tag{A13}$$

Accordingly, the peak amplitude is:

$$A_{\max} = \frac{F_0}{I_0} \times \frac{1}{2D\sqrt{1 - D^2}} \tag{A14}$$

The two vibratory frequencies at which the accelerative vibratory amplitude equals to 0.717 times of the peak amplitude are the two unknowns of the following equation:

$$\frac{F_0}{I_0} \times \frac{x}{\sqrt{(1-x)^2 + 4D^2 x}} = \frac{\sqrt{2}}{2} \frac{F_0}{I_0} \times \frac{1}{2D\sqrt{1 - D^2}} \tag{A15}$$

The Equation (A15) is simplified and rearranged as:

$$\left[2(1 - 2D^2)^2 - 1\right]x^2 - 2(1 - 2D^2)x + 1 = 0 \tag{A16}$$

The above quadric equation has two solutions, x_1, and x_2 that satisfy:

$$\begin{cases} x_1 + x_2 = \dfrac{2(1-2D^2)}{\left[2(1-2D^2)^2 - 1\right]} \\ x_1 \times x_2 = \dfrac{1}{\left[2(1-2D^2)^2 - 1\right]} \end{cases} \tag{A17}$$

By replacing $x_{1/2} = \left(\dfrac{\omega_{1/2}}{\omega_0}\right)^2$, the formulas (A17) are equivalent to:

$$\begin{cases} \left(\dfrac{\omega_1}{\omega_0}\right)^2 + \left(\dfrac{\omega_2}{\omega_0}\right)^2 = \dfrac{2(1-2D^2)}{\left[2(1-2D^2)^2 - 1\right]} \\ \left(\dfrac{\omega_1}{\omega_0}\right)^2 \times \left(\dfrac{\omega_2}{\omega_0}\right)^2 = \dfrac{1}{\left[2(1-2D^2)^2 - 1\right]} \end{cases} \tag{A18}$$

It is noted that:

$$\left(\frac{\omega_1 - \omega_2}{2\omega_0}\right)^2 = \frac{1}{4}\left[\left(\frac{\omega_1}{\omega_0}\right)^2 + \left(\frac{\omega_2}{\omega_0}\right)^2 - 2\left(\frac{\omega_1}{\omega_0}\right)\left(\frac{\omega_2}{\omega_0}\right)\right] \tag{A19}$$

Substitution (A20) into (A19) leads to:

$$\begin{aligned} \left(\frac{f_1 - f_2}{2f_0}\right)^2 = \left(\frac{\omega_1 - \omega_2}{2\omega_0}\right)^2 &= \frac{1}{2}\left\{\frac{(1-2D^2) - \sqrt{2(1-2D^2)^2 - 1}}{2(1-2D^2)^2 - 1}\right\} \\ &= \frac{1}{2}\left\{\frac{(1-2D^2)}{\left[2(1-2D^2)^2 - 1\right]} - \frac{1}{\sqrt{2(1-2D^2)^2 - 1}}\right\} \end{aligned} \tag{A20}$$

Substitution $\alpha_r^{\,2} = \dfrac{1}{1-2D^2}$ and $\dfrac{1}{f_0} = \dfrac{\alpha_r}{f_r}$ into Equation (A20) yields the formula of HPP method:

$$\frac{f_1 - f_2}{2f_r} = \frac{1}{\alpha_r}\sqrt{\frac{\alpha_r^{\,2} - \sqrt{2\alpha_r^{\,4} - 1}}{2\left(2\alpha_r^{\,4} - 1\right)}} \tag{A.21}$$

APPENDIX B – LIST OF SYMBOLS

A	Acceleration amplitude
A_{max}	Maximum acceleration amplitude
c	Damping coefficient
D	Damping ratio
D_{min}	initial (minimum) damping ratio
f_0	Natural frequency
f_r	Resonant frequency
$F_0 \sin \omega t$	Harmonic force
G	Shear modulus

I_0	Moment of inertia of drive system
I	Moment of inertia of specimen
$I_c = 2D^2 I_0$	Virtual damping moment of inertia of the system
I_p	Area polar moment of inertia of circular cross section of specimen
k	Shear stiffness
$k_{equipment}$	Shear stiffness of RC equipment
$k_{specimen}$	Shear stiffness of specimen
L	Specimen height
r	Radial distance from specimen axis
t	Time
T	Resisting torque
V_s	Shear wave velocity
α_r	Ratio of resonant frequency to natural frequency
γ	Shear strain
μ	Material viscosity
θ	Angle of twist
ρ	Mass density of soil
τ	Shear stress
ω	Angular frequency
ω_r	Resonant angular frequency
ω_0	Natural angular frequency
ψ	Phase angle

REFERENCES

Avramidis AS and Saxena SK. "Modified 'stiffened' Drnevich resonant column apparatus," Soils and Foundations 30(3), 53–58, 1990

ASTM: D4015-1992. "Standard test methods for modulus and damping of soils by the resonant-column method," 1995.

Cascante G, Vanderkooy J, and Chung W. "Different between current and voltage measurements in resonant column testing," Canadian Geotechnical Journal 40(3), 806–820, 2003.

Clayton CRI., Priest JA., and Best AI. "The effects of disseminated methane hydrate on the dynamic stiffness and damping of a sand," Géotechnique 55(6), 423–434, 2005.

Drnevich VP. "Recent developments in resonant column testing," in: R. D. Woods (Ed.), Richart Commemorative Lectures, Geotechnical Engineering Division, ASCE, 79–106, 1985.

Drnevich VP, Hardin BO, and Shippy DJ. "Modulus and damping of soils by the resonant column test," in: Dynamic Geotechnical Testing, ASTM STP 654, 91–125, 1978.

Hall RJ and Richart EF Jr. "Dissipation of elastic wave energy in granular soils," Journal of the Soil Mechanics and Foundation Division, ASCE 89(SM 6), 27–56, 1963.

Hardin BO. "The nature of damping of sand," Journal of the Soil Mechanics and Foundation Division, ASCE 11(10), 63–97, 1965.

Hardin BO and Music J. "Apparatus for vibration of soil specimens during triaxial test," in: Instruments and apparatus for soil and rock mechanics, ASTM special technical publication No.392, 55–74, 1965.

Li XS, Yang WL, Shen CK, and Wang WC. "Energy-injecting virtual-mass resonant column system," Journal of Geotechnical and Geoenvironmental Engineering, ASCE 124(5), 428–438, 1998.

Priest AJ. The effect of methane gas hydrate on the dynamics properties of sand. PhD thesis, School of Civil Engineering and the Environment, University of Southampton, 2004.

Richart EF Jr, Hall JR, and Woods RD. Vibrations of soils and foundations, Theoretical and Applied Mechanics series, Prentice-Hall International, Englewood Cliffs, New Jersey, 1970.